JOURNAL OF MATERIALS SCIENCE 28 (1993) 5435–5442

Corrosion study of Al_2O_3 dispersion strengthened Cu metal matrix composites in NaCl solutions

HONGBIN SUN, H.G. WHEAT
Center for Materials Science and Engineering, The University of Texas at Austin, Austin, TX 78712, USA

The corrosion behaviour of alumina dispersion strengthened (DS) copper in 3.5% NaCl solution was studied and compared to the behaviour of pure copper using electrochemical techniques, scanning electron microscopy (SEM), X-ray diffraction, and inductively coupled argon plasma atomic emission spectroscopy (ICP-AES). The corrosion surface products were identified as predominantly copper chloride. It was found that DS copper has similar corrosion characteristics to pure Cu under aerated, open to air and deaerated conditions. The effects of alumina particles and the presence of oxygen in the solutions on the behaviour of the DS Cu were examined. The corrosion mechanism involved is discussed in terms of the roles of the surface CuCl film formation and dissolution during the corrosion process.

1. Introduction

Metal matrix composites (MMCs) basically consist of a reinforcement incorporated into a metallic matrix. By adding elemental, metallic or ceramic reinforcements in various forms, including whiskers, particulates and fibres, to a metal matrix, a composite material is created that may possess superior properties over the monolithic material. In fact, the most important reason to develop MMCs is that they can be tailored to meet the critical performance requirements for advanced engineering applications. These requirements include high strength and stiffness, low densities and low coefficients of thermal expansion. Although the incorporation of the second phase into a matrix material can enhance the physical and mechanical properties of that material, it could also significantly change the corrosion behaviour [1, 2]. Composites, by their nature, combine materials having considerably different corrosion properties. With regard to corrosion resistance, the dual natures of metal matrix composites make them susceptible to three adverse processes [3]: galvanic coupling of the metal and reinforcement; crevice attack at the metal/reinforcement interface; and preferred localized attack at structural and compositional inhomogeneities within the metal matrix.

There is increasing interest in the utilization of Cu metal matrix composite materials for marine applications. In a report to Naval Sea Systems Command, Aylor [4] indicated that of the following materials Al_2O_3/Cu, TiC/Cu, Si_3N_4/Cu, SiC/Cu, B_4/Cu and Gr/Cu, dispersion-strengthened (DS) copper (Al_2O_3/Cu) was the most promising material for high-strength marine applications. In addition, the material's sea water corrosion behaviour in low flow conditions was similar to that of pure copper, while the mechanical properties and modulus were significantly increased over pure copper. Unfortunately, very limited corrosion studies of Cu metal matrix composites in chloride environments have been performed to date. The objective of this research is to study the corrosion behaviour of DS copper (Al_2O_3/Cu) in NaCl solution, focusing on the effects of alumina particles on the corrosion potential, corrosion morphology and corrosion susceptibility of the DS copper, as well as the mechanism involved in the corrosion process. The corrosion behaviour of the monolithic Cu material in NaCl solution was used for comparison.

2. Materials

The materials used in this work consisted of standard ETP copper (99.9% Cu) from Farmer's Copper and DS copper from SCM Metal Products, Inc. DS Cu is produced from a blend of pure copper and aluminium powders. The finely distributed (2.7 vol %) Al_2O_3 particles were achieved by an internal oxidization process. The samples were machined into circular coupons which were 1.6 cm diameter and 0.32 cm thick. Each sample was successively ground using 240, 320, 400 and 600 grit SiC papers followed by alumina powder. Distilled water was used as the lubricant and coolant. After the final polishing procedure, the samples were rinsed in distilled water and then air dried. Fig. 1 shows scanning electron micrographs of the Cu and DS Cu sample surfaces after polishing. Dilute nitric acid solution was used to etch the polished DS Cu sample surface to reveal the particles. Energy Dispersive Spectroscopy (EDS) revealed that the particles shown in Fig. 2 contained Al. The EDS spectrum of particles in Fig. 2 is shown in Fig. 3. While the average particle size of alumina in DS Cu is 3–12 nm,

0022–2461

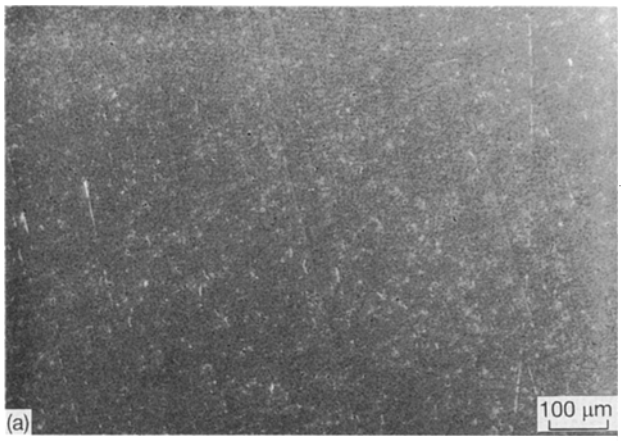

Figure 1 Scanning electron micrographs of (a) pure Cu and (b) DS Cu after polishing. × 100.

Figure 2 Scanning electron micrograph of DS Cu polished and etched using HNO_3 solution. × 10 000.

the finest particle size in Fig. 2 is about 100 nm. Smaller particles cannot be resolved in Fig. 2.

3. Experimental procedure

All electrochemical tests were carried out using the EG&G PAR Potentiostat/Galvanostat Model 273 corrosion measurement system controlled by an IBM Personal System/2 computer and using a standard five mouth flask, a flat specimen holder which exposed a surface area of 1.0 cm^2, a saturated calomel reference electrode and two graphite counter electrodes. Immediately before testing, each specimen was cleaned in

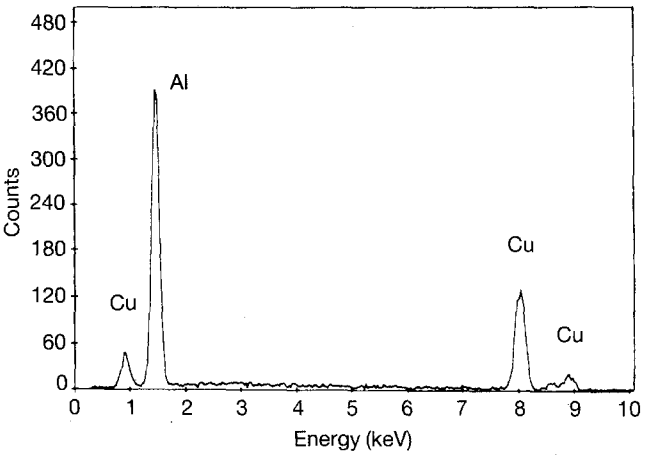

Figure 3 EDS of particles shown in Fig. 2.

distilled water and then air dried. The test solutions were prepared before each test using reagent grade NaCl and distilled water. Both pure Cu and DS Cu samples were tested in 3.5 % NaCl solution under aerated, deaerated and open to air conditions. Before each aerated or deaerated test, oxygen or nitrogen was pumped into the solution for 1 h for aerated and deaerated conditions, respectively. The amount of residual oxygen that existed in the deaerated solution was approximately 1.4 p.p.m., as measured by a dissolved oxygen meter. E_{corr} vs time was measured for up to 22 h. It was found that between 2 and 5 h were required for samples to reach steady state E_{corr} values in the solution. Therefore, the samples were immersed in the solution for 5 h before beginning the tests. At the end of E_{corr} vs time tests, samples were subsequently examined using SEM.

In the potentiodynamic tests, scanning ranges were set from E_{corr} or − 250 mV below E_{corr} to + 800 mV and + 250 mV above E_{corr} or E_{corr} to − 1500 mV for anodic and cathodic polarization, respectively. Tests were run at scan rates of 0.1 and 1 mV s^{-1}. The results that are being reported were done at 1 mV s^{-1}.

In subsequent experiments, potentiostatic tests were performed to determine the current vs time behavior of DS Cu in deaerated and aerated solutions at applied potentials of − 200, − 80, 0, 200 and 600 mV.

SEM studies were performed both before and after electrochemical testing for Cu and DS Cu samples. X-ray diffraction and ICP-AES techniques were used to study the corrosion products.

4. Results and discussions

4.1. E_{corr} vs time tests

Scanning electron micrographs that were obtained after E_{corr} vs time (6 h) experiments are shown in Fig. 4a–d. All cases seem to indicate the presence of a surface film which appears to be evenly distributed over the surface, except in the case of DS Cu under aerated conditions. In this case, the film only partially covers the surface.

4.2. Potentiodynamic studies

4.2.1. Anodic polarization tests

The polarization curves showed certain similarities for

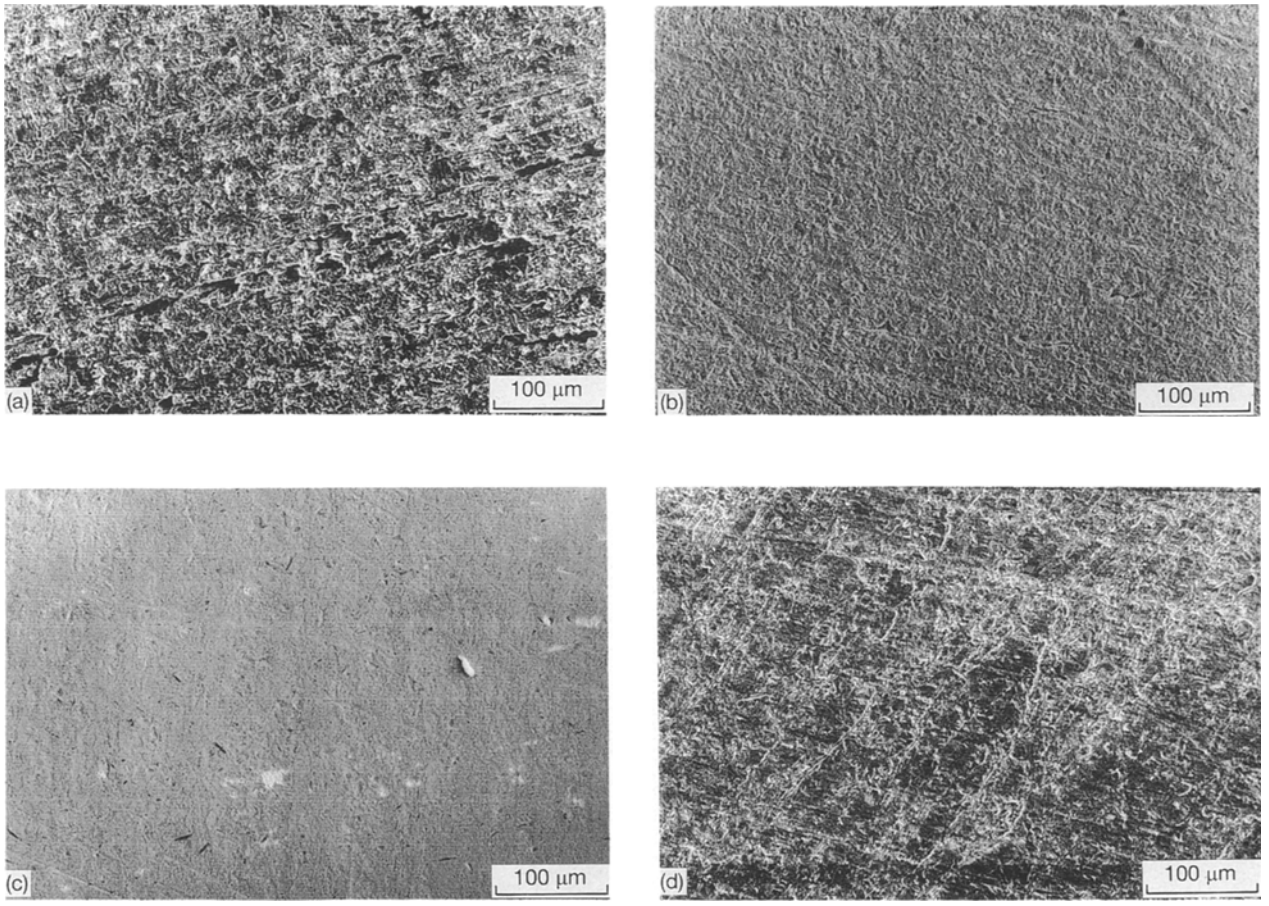

Figure 4 Scanning electron micrographs taken after E_{corr} vs time for 6 h for: (a) pure Cu under aerated conditions, × 200; (b) pure Cu under deaerated conditions, × 200; (c) DS Cu under aerated conditions, × 200; (d) DS Cu under deaerated conditions, × 200.

Cu and DS Cu under all test conditions. Typical anodic polarization curves are shown in Fig. 5. In the potential range examined, there are four distinct regions: the apparent Tafel region (I); the peak current region (II); the current minimum region (III); and the higher potential region (IV). This is similar to results observed by Lee and Nobe [5]. These four regions appeared in the tests started from E_{corr} to about + 800 mV and − 250 mV below E_{corr} to + 800 mV. Under the aerated condition, a secondary peak current appeared in region IV, as seen in Fig 5a. and c.

A model to explain the anodic polarization characteristics of the DS Cu and Cu is proposed based on the transport-reaction mechanism of the Cl^-. Considering the anodic reaction in chloride media [6],

$$Cu + Cl^- = CuCl + e^- \quad (1)$$

$$CuCl + Cl^- = CuCl_2^- \quad (2)$$

the corrosion process involves at least three steps: (a) transport of chloride ions to the DS Cu (or Cu)/NaCl solution interface; (b) Reactions 1 and 2 at the interface; and (c) transport of the corrosion products away from the interface or deposition of the products on the DS Cu or Cu surface. Each of these steps proceeds at a certain rate. At lower potentials (region I), the rate of formation of CuCl is slow compared to the rate of Cl^- transport to the interface and the rate of CuCl dissolution (Equation 2). Therefore, the corrosion process will be limited by the reaction rate in Equation 1 and the product CuCl will be dissolved during the corrosion process. As the potential increases, the potential dependent rate of formation of CuCl will increase. When the CuCl formation rate is higher than its dissolution rate in Reaction 2, excess CuCl will begin to build up on the surface of the DS Cu or Cu samples, which will retard the transport of Cl^- to the interface. At the peak current, the transport of Cl^- becomes rate limiting (region II). The increasing difficulty, as the CuCl film thickens, for Cl^- to reach the DS Cu or Cu metal surface makes the rate of CuCl formation decrease, while its dissolution occurs at a rate that is independent of CuCl film thickness. Thus, there is a current minimum region (III). As the potential increases further, a stable, steady balance between the rates of CuCl formation and dissolution is reached. The film thickness, the dissolution and formation rates and the current in this region (region IV) are then constant and do not vary with time.

By carefully examining the polarization curves for both DS Cu and pure Cu, it is found that the average start potential of region IV is higher for DS Cu than that for pure Cu, as listed in Table I. This can be understood from the model discussed above. The start potential of region IV corresponds to initiation of the balance between the rates of CuCl formation and dissolution. Compared to pure Cu, as shown in Figs 6–8, the corrosion surfaces of DS Cu samples are rougher, due to the dispersed fine alumina particles. The alumina particles on the corroded sample surface make it difficult to cover the surface with CuCl film. In

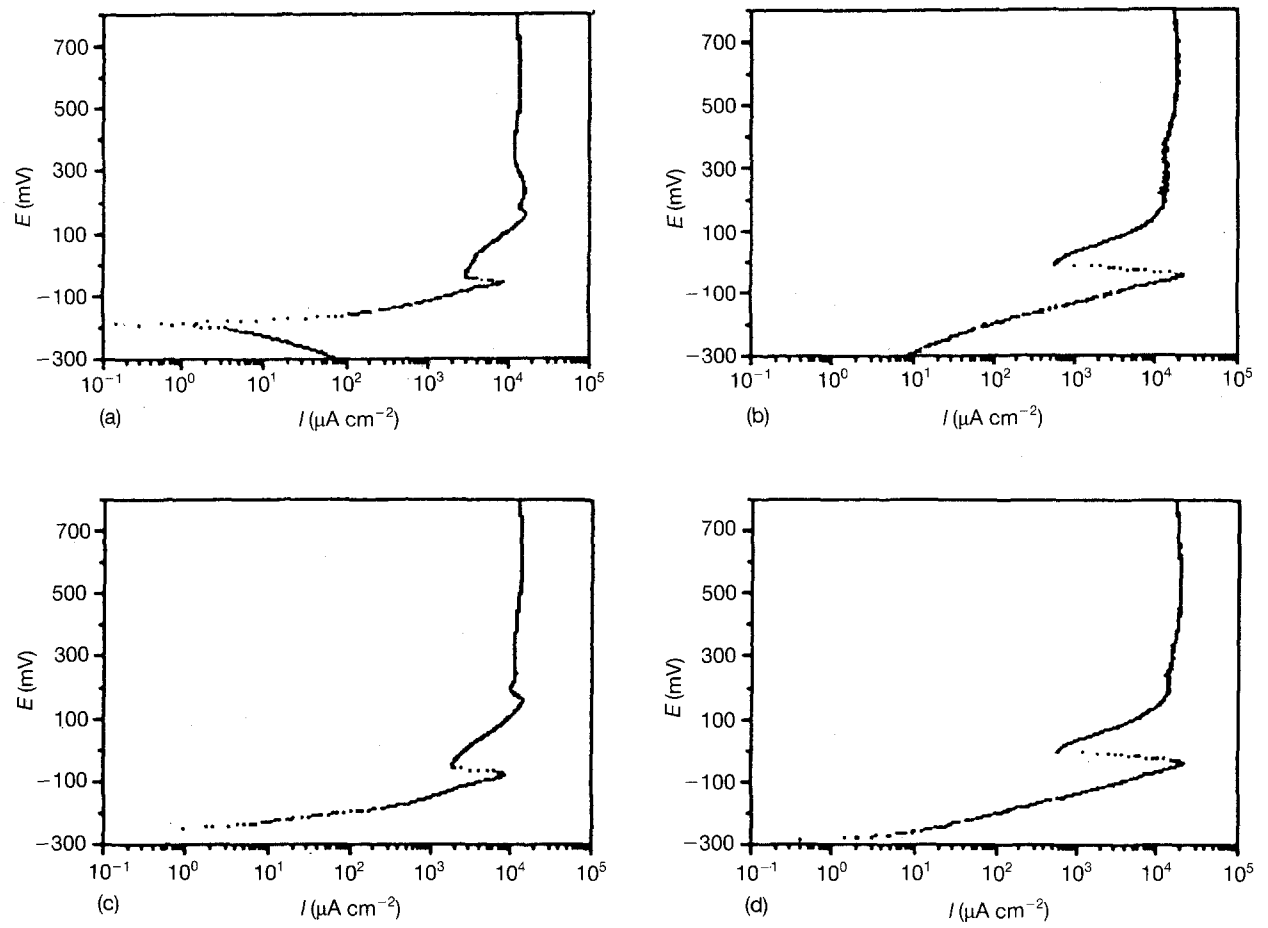

Figure 5 (a) A typical anodic polarization curve of Cu under aerated conditions. (b) A typical anodic polarization curve of Cu under deaerated conditions. (c) A typical anodic polarization curve of DS Cu aerated conditions. (d) A typical anodic polarization curve of DS Cu under deaerated conditions.

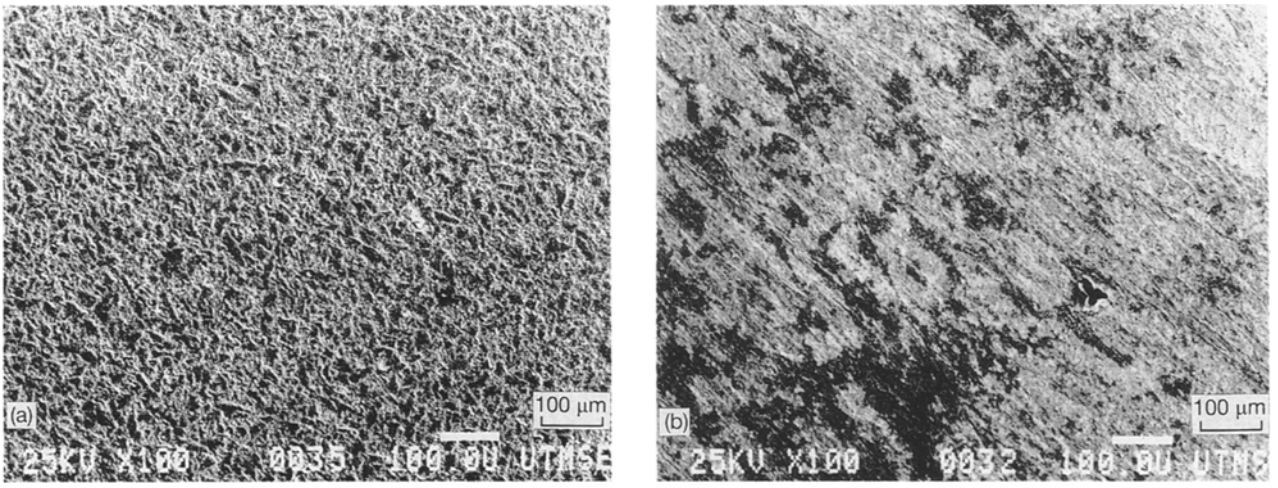

Figure 6 Scanning electron micrographs of (a) pure Cu and (b) DS Cu after anodic polarization under open to air conditions. × 100.

other words, a thicker film is required to cover the surface to the extent of the smooth pure surface, which means a higher potential is required for the DS Cu to reach region IV.

TABLE I The start potentials of region IV (mV vs SCE)

	DS Cu	Cu
Deaerated	170	160
Aerated	212	210

Table I also indicates that the start potentials of region IV for both Cu and DS Cu are higher in aerated chloride solutions than in deaerated chloride solutions. In chloride media containing dissolved oxygen, the electroreduction of the oxygen shifts the equilibrium of the $Cu/CuCl_2^-$ reaction (combination of Equations 1 and 2):

$$Cu + 2Cl^- = CuCl_2^- + e^- \quad (3)$$

at the copper–solution interface so that a much higher interfacial concentration of $CuCl_2^-$ is obtained than in

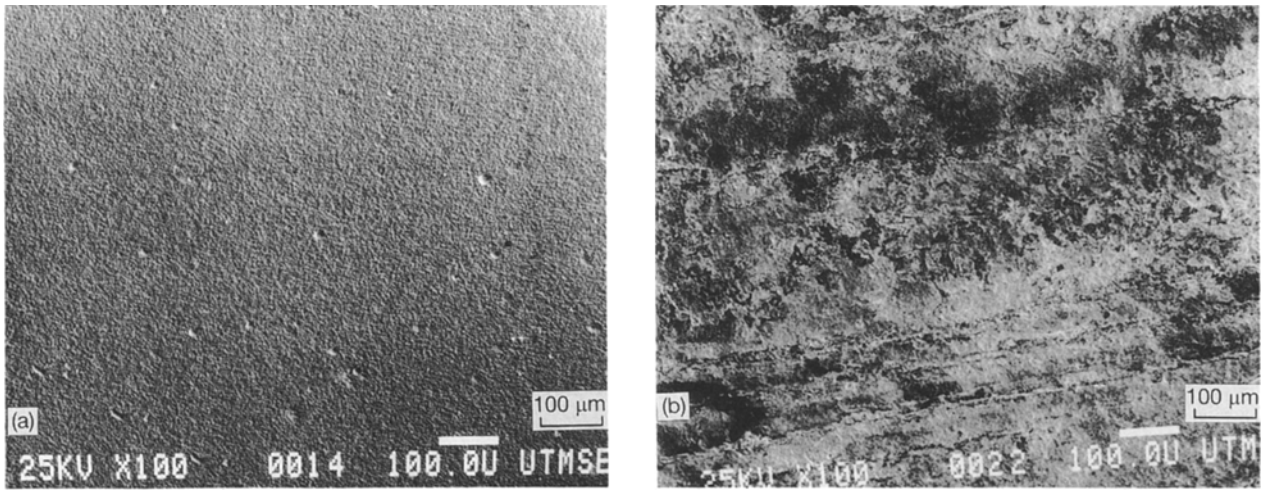

Figure 7 Scanning electron micrographs of (a) pure Cu and (b) DS Cu after anodic polarization under aerated conditions. × 100.

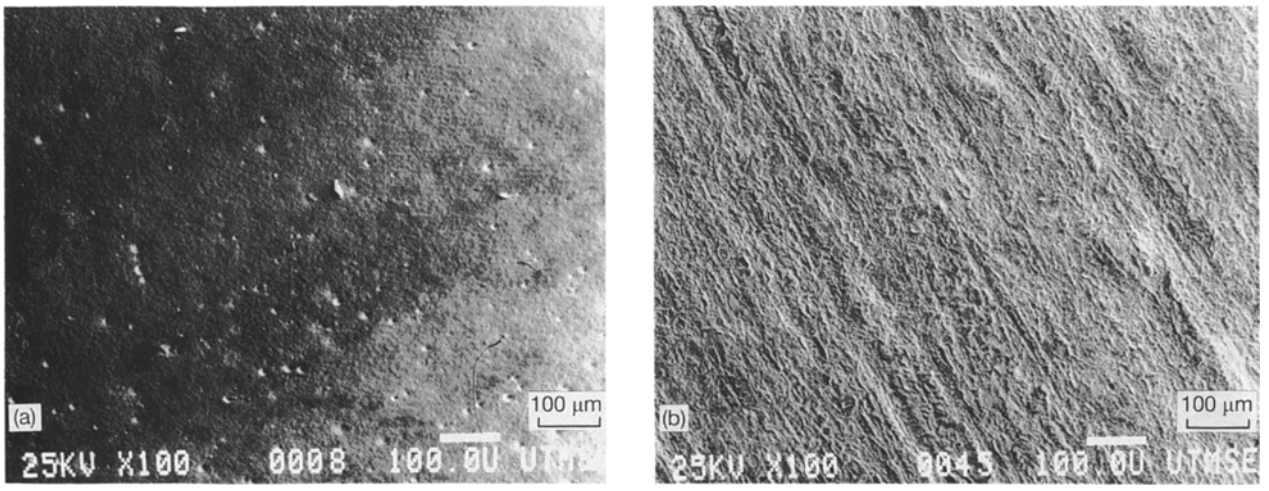

Figure 8 Scanning electron micrographs of (a) pure Cu and (b) DS Cu after anodic polarization under deaerated conditions. × 100.

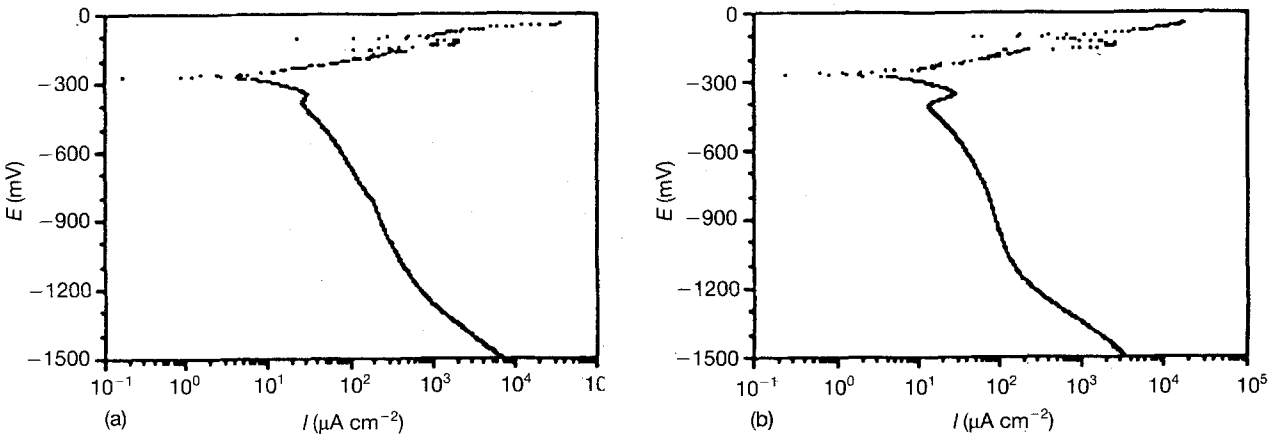

Figure 9 A typical cathodic polarization curve of (a) Cu and (b) DS Cu under deaerated conditions.

the absence of oxygen. This then leads to the increased dissolution rate of CuCl (Equation 2) and thus higher start potentials are required for the balance between the formation and dissolution of the CuCl.

4.2.2. Cathodic polarization tests

Typical cathodic polarization curves of Cu and DS Cu under deaerated condition are shown in Fig. 9. Two cathodic peaks were observed. The second peak immediately follows the first cathodic peak. Bjorndahl and Nobe [6] suggested that the cathodic peaks were caused by CuCl reduction (Equation 2) and the oxygen reduction reaction

$$O_2 + H_2O + 4e^- = 4OH^- \quad (4)$$

4.3. Potentiostatic studies

In order to gain more insight into the corrosion process, potentiostatic tests were performed at several

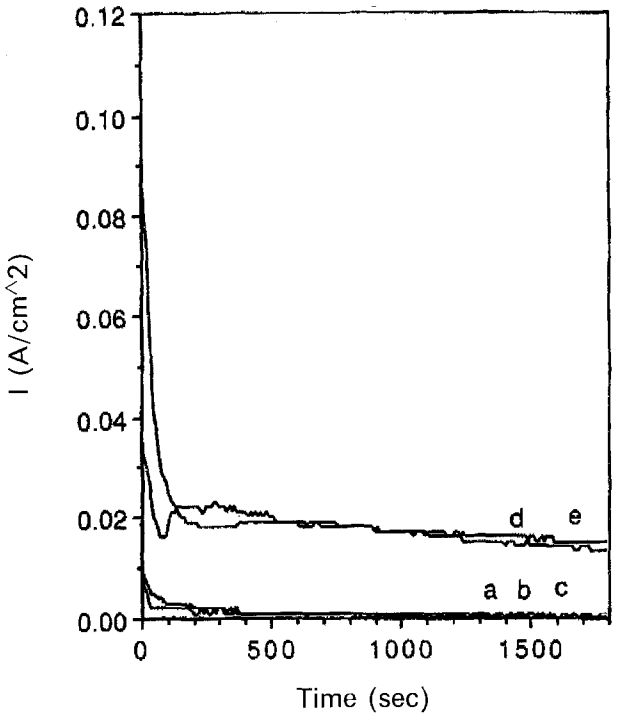

Figure 10 Potentiostatic curves of DS Cu under aerated conditions at applied potentials of (a) − 200 mV, (b) − 80 mV, (c) 0 mV, (d) 200 mV and (e) 600 mV.

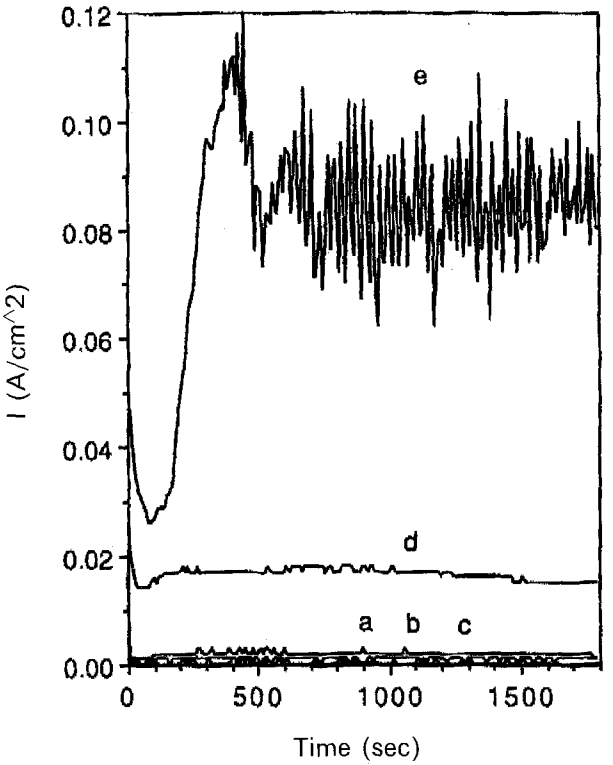

Figure 11 Potentiostatic curves of DS Cu under deaerated conditions at applied potentials of (a) − 200 mV, (b) − 80 mV, (c) 0 mV, (d) 200 mV and (e) 600 mV.

applied potentials for 30 min after a 2 h delay. While tests were conducted for both aerated and deaerated conditions, the most definitive results were obtained under aerated conditions. Fig. 10 shows the potentiostatic curves under aerated conditions. For a − 200 mV applied potential, which is in the Tafel region (I), the current density oscillates between 0 and 1000 $\mu A\,cm^{-2}$. For − 80, 0, 200 and 600 mV applied potentials, the current density decreased to a value that was dependent on the applied potential and then levelled off. Under deaerated conditions, as shown in Fig. 11, the current density oscillated between 0 and 1000 $\mu A\,cm^{-2}$ for − 200 and − 80 mV applied potentials. The current density decreased first and then levelled off for 0 and 200 mV applied potentials. For a 600 mV applied potential, which is in the plateau current region (IV), current oscillations occurred and the oscillating amplitude changed with time. Because the balance between film formation and dissolution is dynamic, there is an instability in the corrosion process. It is believed that this oscillation is due to the instability of the surface film [7].

The corrosion surfaces that were obtained after the potentiostatic tests under aerated conditions were examined using SEM. Fig. 12 shows the SEM microphotographs of the corrosion surfaces under aerated conditions and it is clear that the corrosion process can be followed by observing these microphotographs. At an applied potential of − 200 mV, the surface appears to be partially covered by a surface film. The coverage increases at a potential of − 80 mV (around the peak current density) and at an applied potential of 0 mV (around the minimum current) the film seems to completely cover the surface. At an applied potential of 200 mV, coarsening of the surface film is observed and at an applied potential of 600 mV, part of the outer film seems to have been removed. In fact, Fig. 12 shows remnants of the film morphologies that existed at applied potentials of 0 and 200 mV. This could be indicative of the fact that at the higher potentials, some of the surface film had fallen off. Therefore, the outer surface may have been in the process of reforming over the entire surface and may have required more time. In fact, in one sample which was subjected to an applied potential of 600 mV vs SCE under deaerated conditions for 18 h, the sample surface was covered by a thick film. The insoluble corrosion products on that surface were identified by X-ray diffraction right after the test and were determined to be primarily copper chloride (CuCl). Fig. 13 shows the X-ray diffraction spectrum of that product. It should be mentioned that massive amounts of residue were observed in the solutions following potentiostatic testing at 600 mV. They were identified by ICP-AES as Cu and chloride. All these results are consistent with the electrochemical test results.

4.4. The Tafel constant, polarization resistance, corrosion rate and E_{corr} values

The anodic and cathodic Tafel constants, polarization resistance values, corrosion rates and E_{corr} values for all test conditions were obtained from the polarization tests and are listed in Table II.

The experimental observations are the following.

1. The polarization resistance values for pure Cu are lower than those for DS Cu under all conditions.

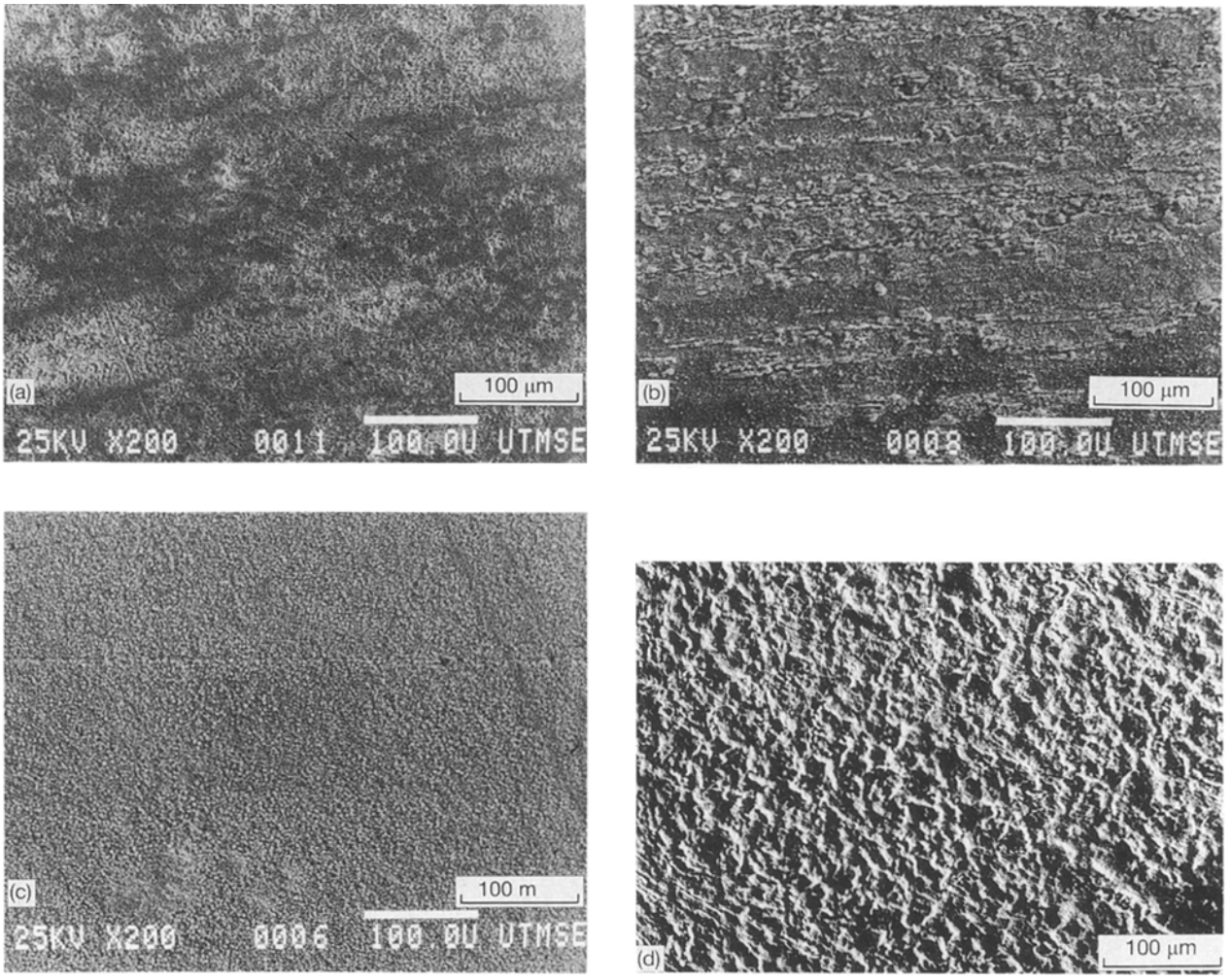

Figure 12 Scanning electron micrographs of DS Cu after potentiostatic tests for 30 min under aerated conditions at applied potentials of (a) − 200 mV, (b) − 80 mV, (c) 0 mV, (d) 200 mV and (e) 600 mV. × 200.

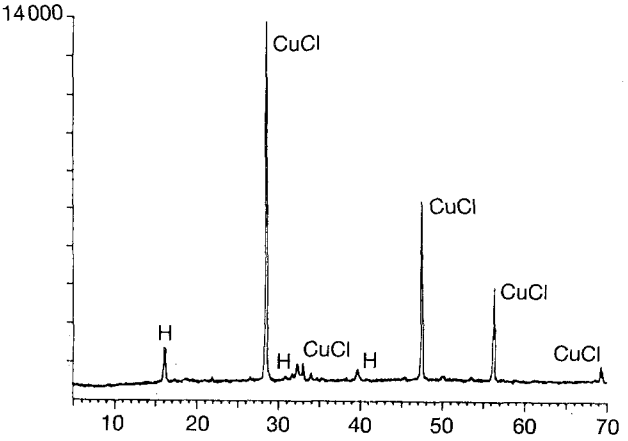

Figure 13 X-ray diffraction spectrum of the corrosion surface film.

2. The E_{corr} values are more active as the amount of oxygen decreases and they are slightly more active for DS Cu than for pure Cu.

3. The corrosion rate in aerated conditions is higher than that in deaerated conditions.

4. The polarization resistance in aerated conditions is lower than that in deaerated conditions.

The results concerning the effect of oxygen on the corrosion behaviour of Cu are consistent with previous investigations (e.g. Bjorndahl and Nobe [6]). They measured the rotation disc rate, ω, in aerated and deaerated conditions and determined the polarization resistance, R_p, using $R_p \sim 1/\omega^{1/2}$. Their results indicates that the corrosion rate of copper in aerated chloride solution is higher than that in deaerated solution. This can be explained using the discussion in the last paragraph in section 4.2.1.

TABLE II Tafel Constants, R_p, and mpy Values for Cu and DS Cu

Conditions	Parameters		Cu	DS Cu
Aerated	Tafel	Anodic	41.49	72.57
	(mV)	Cathodic	181.62	108.95
	R_p (k-ohms cm^2)		4.2827	6.66
	Ecorr (mV vs SCE)		− 204	− 220
	Corrosion rate (mpy)		1.90	1.51
Air	Tafel	Anodic	61.84	56.31
	(mV)	Cathodic	115.44	101.38
	R_p (k-ohms cm^2)		4.2841	4.5245
	Ecorr (mV vs SCE)		− 223	− 247
	Corrosion rate (mpy)		2.35	2.397
Deaerated	Tafel	Anodic	109.1	71.76
	(mV)	Cathodic	108.18	358.19
	R_p (k-ohms cm^2)		7.39	9.2649
	Ecorr (mV vs SCE)		− 290	− 298
	Corrosion rate (mpy)		1.37	1.506

From these observations, it seems that the DS Cu has a corrosion resistance that is comparable to or slightly better than that of Cu. It is noted that E_{corr} is more active for DS Cu than Cu. One possible reason for this is that the DS Cu may have a higher initial susceptibility to corrode compared to pure Cu because of the presence of Al_2O_3 particles. DS Cu may corrode in the interfacial area due to the residual stresses or galvanic corrosion between the alumina particles and the copper matrix. In other words, even though it may be easy to initiate corrosion in DS Cu, it may not necessarily have a higher corrosion rate than Cu, because corrosion rates depend on the corrosion process. Therefore, DS Cu has comparable corrosion resistance to pure Cu after the protective film is formed on the surface, even though its E_{corr} is more active than that for Cu. This result was also observed by Aylor [4] in their tests of marine exposures for Cu and DS Cu for 1–7 months. The calculated corrosion rates based on the linear polarization testing showed that the corrosion rates for DS Cu were initially higher than for pure copper during the first month, but the rates for the composites decreased to rates that were comparable to copper after 3.5 months.

5. Conclusions

Electrochemical test results showed that the DS Cu has similar corrosion characteristics compared to Cu under aerated, deaerated and open to air conditions. The alumina particles in the DS Cu, however, do affect the corrosion behaviour of the DS Cu. The insoluble corrosion products on the samples are primarily copper chloride, as determined using X-ray diffraction and ICP-AES. The corrosion films at different regions of the polarization curve were studied using SEM. The results showed that the corrosion process is controlled by the formation and dissolution of the surface film. The alumina particles on the corroded surface affect the coverage of the CuCl film. Thus the particles play an important role in the corrosion process of the DS Cu. By dividing the corrosion behaviour into initiation and development and combining the results from chemical analysis of the surface film formed on DS Cu during the corrosion process, one can explain the observed different anodic and cathodic Tafel constants, polarization resistance values, corrosion rates and E_{corr} values for DS Cu and pure Cu.

Acknowledgement

The authors wish to thank the Office of Naval Research, Project N00014-89-J-3116, for financial support of this work.

References

1. R. C. PACIEJ and V. S. AGURWALA, *Corrosion* **42** (1986) 718.
2. H. SUN, E. KOO and H. G. WHEAT, *ibid.* **47** (1991) 742.
3. P. P. TRZASKOMA, *J. Metals* **Dec.** (1988) 21.
4. D. M. AYLOR, "Development of copper–base metal matrix composites materials", DTNSRDC/SME-85/10, David Taylor Naval Ship R&D Center (1985).
5. H. LEE and K. NOBE, *J. Electrochem. Soc.* **133** (1986) 2035.
6. W. D. BJORNDAHL and K. NOBE, *Corrosion* **40** (1984) 82.
7. H. LEE, K. NOBE and A. PEARLSTEIN, *J. Electrochem. Soc.* **132** (1985) 1031.

Received 24 September
and accepted 19 November 1992